

ANALYSIS AND SIMULATION OPTIMIZATION OF CONNECTING ROD CAP FAILURE IN COMPRESSOR

Zhao, C. L.*; Huang, Y.**.#; Wu, S. H.***; Yu, L.*; Dong, J. Y.**** & Yi, Q. C.*

* Geely University of China, Chengdu 641423, China

** Tianfu College of SWUFE, Mianyang 621000, China

*** Sichuan Technology & Business College, Chengdu 611730, China

**** Chengdu HaiRui Product Quality Technology Test Co. LTD, Chengdu 641423, China

E-Mail: huangyi@tfswufe.edu.cn (# Corresponding author)

Abstract

The connecting rod cap is one of the key components for the reciprocating motion of compressors and internal combustion engines, and it works in conjunction with the connecting rod to convert power. Regarding the fracture problem of the connecting rod cap of a certain compressor, the initial cause of the fracture was preliminarily determined through physical and chemical analysis to be the excessively small fillet radius at the bolt installation plane. A finite element model was established to verify the cause of the fracture, and based on this as a comparison benchmark, the model structure was optimized. It was found that increasing the fillet radius could indeed improve the performance of the connecting rod cap, but it is not the case that the larger the fillet radius, the better. In the simulation, it was discovered that the performance of the fillet with a radius of 4.5 mm was significantly worse than that of the fillet with a radius of 3.5 mm. Therefore, in the design of the connecting rod cap, an appropriate fillet radius should be selected to ensure its good performance. Additionally, a design combining the fillet with a chamfer can also be considered.

(Received in August 2025, accepted in October 2025. This paper was with the authors 1 month for 1 revision.)

Key Words: Connecting Rod Cap, Failure, Physical and Chemical Analysis, Simulation Optimization

1. INTRODUCTION

The reciprocating piston compressor works in a similar way to an automotive engine. It uses the reciprocating linear motion of the piston in the cylinder to cause periodic changes in the cylinder volume, thereby completing the four working stages of intake, compression, exhaust, and clearance expansion. The typical moving parts include the crankshaft, connecting rod, piston assembly, and intake and exhaust valves. The connecting rod cap, in conjunction with the connecting rod, ensures the periodic motion of the piston. In related engineering applications, it has been found that the failure probability of the connecting rod cap is higher than that of other moving parts. Therefore, studying the causes of failure and structural optimization of the connecting rod cap is of great significance for the improvement of gas compressors.

Similar research was conducted as early as 2017. Zhu et al. used physical and chemical analysis methods and finite element simulation methods to conduct a systematic analysis of similar parts and concluded that the failure of their research object was due to the excessively small transition fillet R [1]. In this study, although the structure of the research object was significantly improved, especially by independently designing the bolt connection plane to avoid the overlap of the arc surface and this plane, the same part failure still occurred. Therefore, it is necessary to conduct a similar type of research to further verify the failure cause and provide more effective and specific suggestions for the optimization and improvement of similar parts. This study mainly completed the following work:

(1) A working model of the relevant institutions was established, and the working state of the reciprocating piston compressor was systematically analysed, providing a direction for finite element simulation.

(2) Based on physical and chemical analysis methods, the failure cause of the connecting rod cap was initially judged. Then, a failure model was reconstructed through finite element simulation, and the failure cause of the connecting rod cap was verified.

(3) After systematically analysing the failure cause of the connecting rod cap, this study specifically optimized and improved the structure of the connecting rod cap. The results of the structural optimization were verified again through finite element simulation software. The optimization results showed that the performance of the improved connecting rod cap was significantly enhanced under the same working conditions, and the structural improvement was effective.

(4) In the specific structural improvement plan, two structural improvement schemes were verified. The first one was optimized by increasing the fillet, and the second one was optimized by changing the fillet to a bevel. The relevant simulation verification indicated that both structural improvements could effectively enhance the structural performance of the connecting rod cap.

2. RELATED WORKS

At present, there are relatively few studies specifically targeting the key components of natural gas compressors, such as the connecting rod cap. Most research focuses on the connecting rod. Petrova and Filimonov observed fatigue crack events in the piston head of the connecting rod in the compressor during operation. To assess the possibility of its trouble-free operation, they determined the values and nature of the load changes affecting the crank mechanism of the compressor during operation through numerical experiments and revealed the section with the maximum load [2]. Wang et al. studied the wear of the crankshaft connecting rod in a refrigerator compressor. The results showed that there was abrasive wear and adhesive wear on the surfaces of the crankshaft and connecting rod. They proposed process control measures and designed a composite surface treatment process for the crankshaft based on its failure mechanism and production process and conducted bench tests [3]. Cetin and Okur proposed a new design to address the unnecessary motion of the piston due to secondary motion in the traditional crank connecting rod mechanism, which leads to problems such as noise, vibration, gas leakage, friction, and wear in the system. They compared and analysed this design with the traditional mechanism and verified it using a finite element analysis model [4]. Li et al. proposed a quantitative diagnostic method for the loosening of the threaded connection of the piston rod in a hydrogen reciprocating compressor to prevent accidents caused by piston rod fractures. Based on the Hilbert transform, they used variational mode decomposition and data dimension reduction to form a multi-band feature spectrum, which demonstrated satisfactory performance in preserving the features of time-domain and frequency-domain acceleration signals and compressing the spectrum [5]. Peng and Huang derived the expression for the instantaneous inertia of the crank-connecting rod-piston mechanism and established a differential equation for the torsional vibration of the shaft system considering the variable inertia of the cylinder and nonlinear friction. The relative error between the numerical model calculation and the experimental data was 8.2 %, indicating that the numerical model has good calculation accuracy [6]. Li et al. considered the influence of the friction between the piston and the cylinder on the instantaneous inertia of the crank connecting rod mechanism and established a nonlinear torsional vibration dynamics model for the shaft system of a shale gas compressor. After considering the friction between the piston and the cylinder, the second-order natural frequency of the shaft system showed a "high-low-high" fluctuation pattern; as the friction coefficient increased, the amplitude and peak vibration velocity of the shaft system increased [7]. Wang et al. proposed a calculation and suppression method for the torsional vibration of the crankshaft system in large multi-column compressors, especially under variable loads and multiple working conditions, to

reduce the torsional vibration of the compressor crankshaft and ensure the safe and stable operation of the compressor unit [8].

In addition, research on the overall performance and fault diagnosis of compressors is also an important direction. For instance, non-destructive fault detection technology that determines whether equipment is normal based on mechanical abnormal signals [9, 10]. Hou and Pan proposed and implemented the Teager-Kaiser energy operator and envelope spectrum analysis technology for the fault detection of reciprocating compressor discharge valves. By effectively characterizing the instantaneous frequency and amplitude of the discharge valve signal based on energy recognition, characteristic signals can be extracted and noise eliminated [11]. Kowalczyk et al. conducted performance tests on linear compressors under power supply voltages of 190–265 V and power supply frequencies within the range of 45–65 Hz, combined with inverters to achieve performance modulation. The results were compared with those of reciprocating compressors with similar displacements, and the power consumption of linear compressors was found to be on average twice as low as that of reciprocating compressors [12]. Lu et al. used digital twin technology and proposed a method for constructing a digital twin model of reciprocating air compressors based on surrogate models. The surrogate model was constructed based on the physical information long short-term memory neural network (PILSTM). Regularization formulas were added based on the characteristics of cylinder pressure changes to ensure the smoothness of the predicted pressure [13]. Elagin and Khmelev proposed a mathematical model for reciprocating compressors, which is based on thermodynamic methods for open systems, mechanical laws describing the relative motion of reciprocating motion units, laws controlling the motion of the system's centre of mass, and the motion of the system relative to the centre of mass [14]. Deng et al. addressed the issue that the inter-stage volume provided by the intercooler in micro multi-stage reciprocating compressors is often insufficient due to size limitations. They conducted numerical analysis on the thermodynamic characteristics within the cylinder and the intercooler by establishing a stage series thermodynamic model and experimentally studied the performance of the compressor by changing the diameter of the intercooler channel [15].

3. RESEARCH METHOD

3.1 Physical and chemical analysis methods

Through morphological observation, scanning electron microscopic analysis, dimensional analysis, metallographic structure observation, mechanical property testing, and chemical composition testing of the compressor connecting rod cap, the failure cause of the part was preliminarily judged to find the fundamental mechanism of the fracture of the compressor connecting rod cap. Then, combined with finite element analysis, the failure cause was verified to ultimately determine the failure cause of the compressor connecting rod cap. In the morphological analysis stage, the macroscopic features of the fracture surface were detailly characterized through visual inspection, such as the crack initiation position, propagation path, and fracture surface morphology, which can objectively determine the fracture mode and provide a basis for subsequent analysis. Electron microscopy deeply analysed the microscopic features of the fracture, precisely identifying the source area, propagation area, fatigue striations, or brittle characteristics of the fracture surface, providing key evidence for revealing the structural defects of the connecting rod cap, especially the location and severity of stress concentration areas. Metallographic structure observation, mechanical property testing, and chemical composition detection focused on the assessment of internal material defects, including non-metallic inclusions and improper heat treatment processes, such as inaccurate control of quenching temperature leading to coarse grains or composition deviations. These factors significantly affect the phase composition and grain boundary state

of the microstructure of the material; mechanical property analysis selected samples to determine the tensile strength, yield strength, and other indicators of the material. Through systematic analysis of the direct causes of failure occurrence [16, 17], the completeness and reliability of the analysis conclusion were ensured.

3.2 Finite element analysis and optimization methods

The finite element analysis method is a type of numerical simulation technology and has now been widely applied in the reliability simulation of mechanical structures due to its high efficiency and high calculation accuracy. By constructing an accurate finite element model, the stress and strain distribution of the connecting rod cover under complex working conditions and possible failure situations can be simulated, thereby providing data support for subsequent structural improvements. The connecting rod cover of a reciprocating compressor, together with the connecting rod, cylinder piston, cylinder block, and crankshaft, forms the main working structure of the compression system. A typical structure is shown in Fig. 1. Since the main structure mainly performs reciprocating motion, based on the movement law of the compressor cylinder, the overall structure can be simplified as the reciprocating motion of a crank-slider, and its motion schematic diagram is shown in Fig. 2.

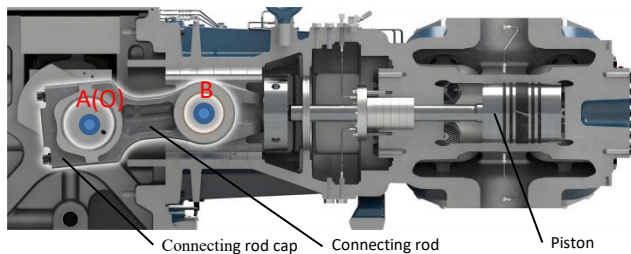


Figure 1: Typical structure of a compressor.

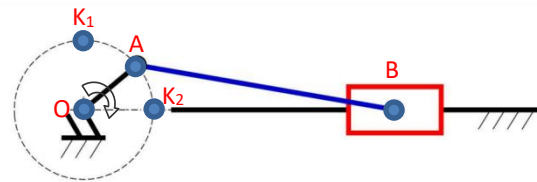


Figure 2: Simplified structure diagram.

The main working principle of reciprocating compressors is that the motor drives the crankshaft to rotate, and the piston is driven to move back and forth periodically in the cylinder wall through the connecting rod. The entire ideal working cycle is divided into three parts: intake, compression and exhaust. During these three stages, in the compression stage, as the piston changes direction under the drive of the crankshaft, that is, when point A moves from k_1 to k_2 , the piston moves to the right and the intake valve closes. The volume of the working space decreases, and the pressure inside the cylinder continuously rises until it reaches the rated pressure. According to Newton's third law, the force is mutual, so the load on the connecting rod cover at this time should be the largest and is the most likely to fail. Therefore, when conducting finite element analysis, the compression stage is taken as the sample, and the constraint conditions of the connecting rod cover are established, and the driving conditions are applied. At this time, the piston, connecting rod, crankshaft and connecting rod cover are on the same straight line, and these components are simplified into one rigid body. The load of the compressed air will directly act on the connecting rod cover. At this time, there should be tensile force acting on the four connecting bolts between the connecting rod cover and the connecting rod. The simplified model is shown later in Fig. 15.

4. EXPERIMENTAL ANALYSIS AND OPTIMIZATION

4.1 Physical and chemical analysis

(1) Morphological analysis

The fracture location of the connecting rod cap is at the transition R position of the connecting rod screw installation surface, where there is a significant stress concentration

feature. The fracture surface shows typical fatigue expansion arc patterns (fatigue striations), and the crack source area is located on the transition R surface area. The fatigue crack radiates outward and eventually leads to instantaneous fracture. The specific morphological features are shown in Figs. 3 a and b. Both of the two fractured connecting rod screws have significant necking near the fracture surface, and obvious plastic deformation marks can be seen at the root of the thread. The fracture surface presents a dimple morphology, which conforms to the macroscopic characteristics of single overload fracture, indicating that the connecting rod screw experienced a one-time ductile fracture under tensile stress. The fracture morphology is detailed in Fig. 3 c.

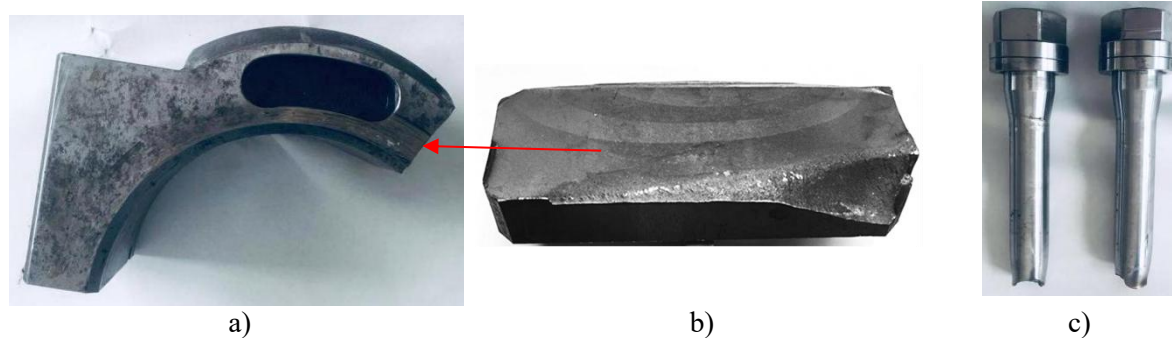


Figure 3: The state of fracture.

(2) SEM analysis

Through scanning electron microscopy analysis of the fracture surface, the results show that area A is clearly identified as the fatigue origin zone of the fracture surface. The fatigue source area presents a clear linear fatigue source morphology, which strongly indicates that stress concentration is the main driving factor for fatigue origin, belonging to the typical fatigue origin characteristics dominated by stress concentration. Relevant images can be seen in Figs. 4 to 6. Further examination reveals that no slag inclusions, voids or other metallurgical defects are observed on the fracture surface, indicating good metallurgical quality of the material. Area B is defined as the fatigue propagation zone, and the fatigue propagation striation features can be clearly observed in the microstructure, which present regular spacing and direction, reflecting the typical process of periodic crack propagation. Specific details are shown in Figs. 7 to 8. Area C also belongs to the fatigue propagation zone, and the fatigue propagation striation features are clearly visible in the microstructure, which are consistent with those in area B, showing stable crack propagation behaviour. Relevant images are shown in Figs. 9 to 10. Special note: 12 \times , 15 \times , 20 \times , 100 \times , and 500 \times refer to magnification.

As the fracture originated at the transition R position of the connecting rod screw installation surface, to comprehensively assess the structural integrity of the connecting rod cover, the other side transition R of this connecting rod cover was dissected, and its dimensions were inspected. After dissection, it was found that a crack about 16 mm deep also appeared at this transition R position, starting from the transition R and extending inward, as shown in Fig. 11.



Figure 4: Schematic diagram of fracture zone partitioning.

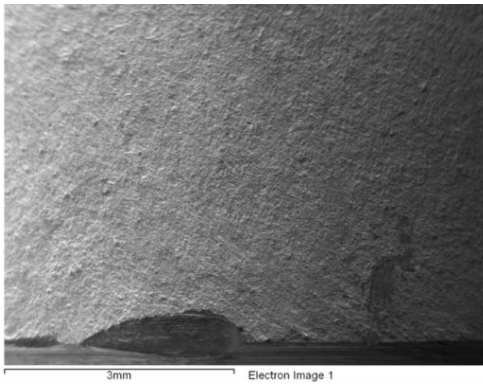


Figure 5: Fracture morphology in area A (20×).

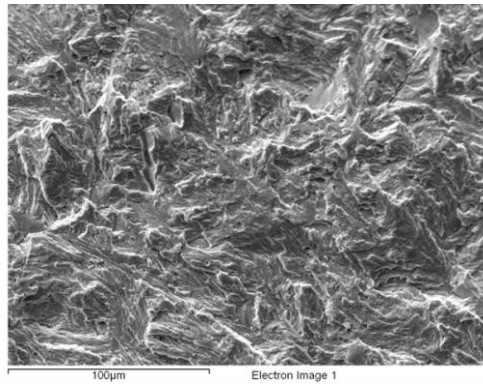


Figure 6: Fracture morphology in area A (500×).

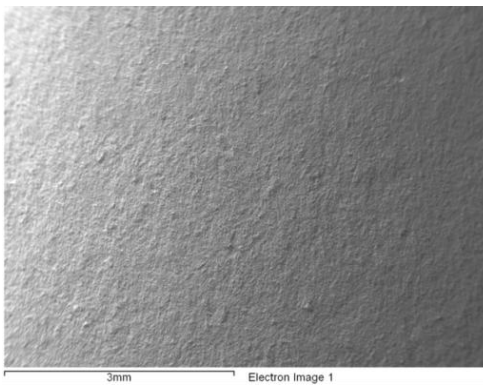


Figure 7: Fracture morphology in area B (20×).

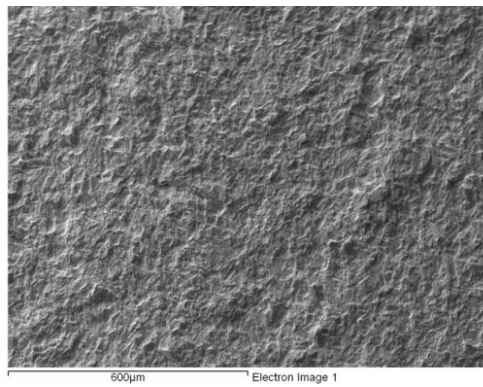


Figure 8: Fracture morphology in area B (100×).

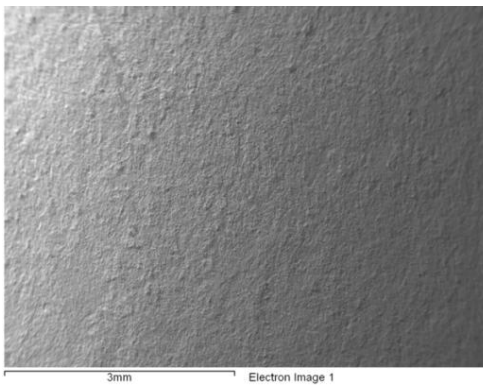


Figure 9: Fracture morphology in area C (20×).

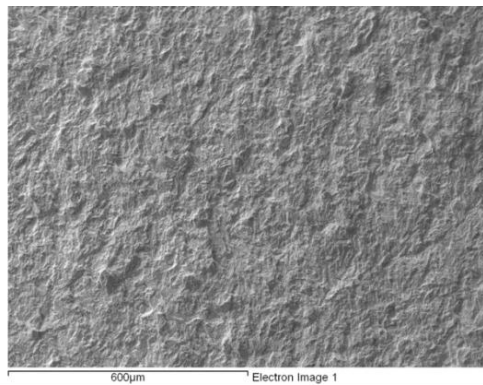


Figure 10: Fracture morphology in area C (100×).

(3) Transition R size inspection



Figure 11: Cracks that occur at the transition R position on the other side.

Furthermore, a dimensional inspection of the transition R was carried out to provide parameters for subsequent dimensional optimization. The magnification used was 12× and 15×. After inspection, the size of the transition R was approximately 2.50 mm, as shown in Figs. 12 and 13.

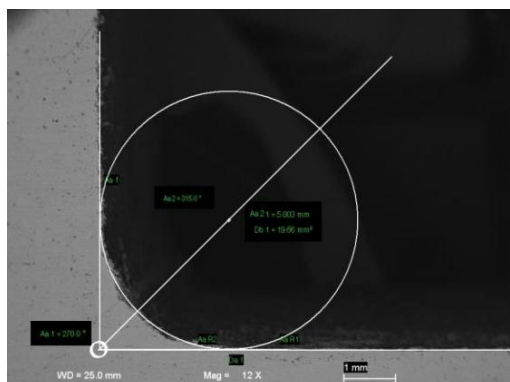


Figure 12: Transition R size (12×).

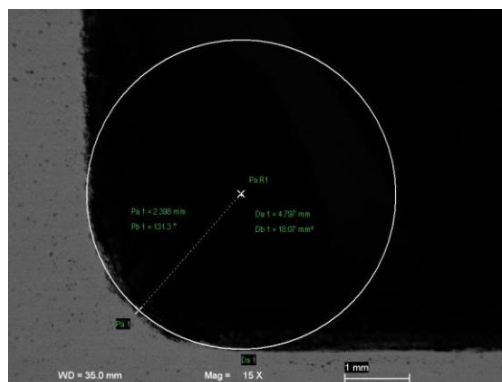


Figure 13: Transition R size (15×).

(4) Metallographic analysis

Near the fracture surface of the connecting rod cover, samples were extracted using the standard metallographic sampling method and detailed microstructure observation was conducted with a metallographic microscope at a magnification of 500×. The inspection results showed that the microstructure near the fracture was tempered upper bainite, with no inclusions or abnormal deformations found. This is in line with the material heat treatment specifications, indicating a normal microstructure state and no typical material defects [18]. For specific details, please refer to Fig. 14.

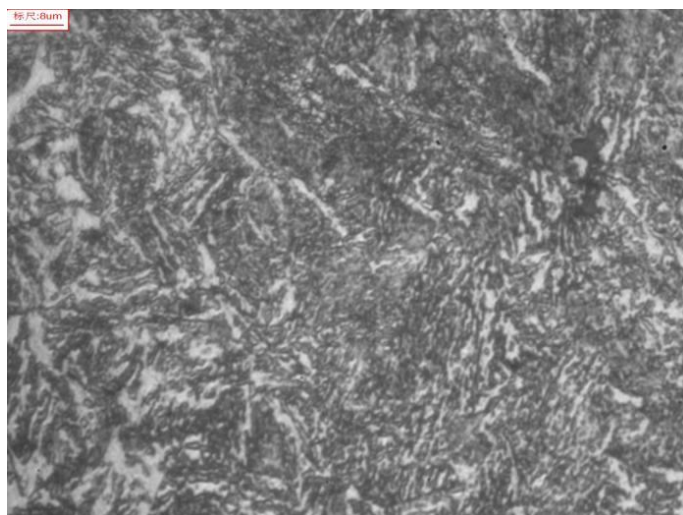


Figure 14: Metallographic structure (500×).

(5) Mechanical property

Mechanical property tests were conducted on samples taken from the middle of the arc-shaped position of the connecting rod cover. The results are shown in Table I.

Table I: Mechanical properties of connecting rod caps.

Strength of extension R_m (MPa)	Yield strength $R_{0.2}$ (MPa)	Elongation after fracture A (%)	Post-fracture shrinkage rate Z (%)	KV2 impact energy (J)		
				1	2	3
902	702	14.0	42.0	16.2	16.7	18.0

(6) Chemical component analysis

Representative samples were selected from the area near the fracture of the connecting rod cover and subjected to detailed chemical composition analysis using spectral analysis. The analysis results show that the content of each element in the material of the connecting rod cover strictly complies with the chemical composition requirements for 42CrMo material stipulated in the Chinese national standard GB/T 3077-2015, including key elements such as carbon, chromium, and molybdenum, all within the specified range. The test data are detailed in Table II.

Table II: Chemical composition of connecting rod covers.

Project	C (%)	Si (%)	Mn (%)	P (%)	S (%)	Cr (%)	Mo (%)
Observed value	0.40	0.29	0.63	0.013	0.003	0.96	0.18
Standard values	0.38~0.45	0.17~0.37	0.50~0.80	≤0.03	≤0.03	0.90~1.20	0.15~0.25

4.2 Results of physical and chemical analysis

From the macroscopic analysis of the fracture surface and the results of scanning electron microscopy, it can be seen that the fracture of the connecting rod cover is a typical fatigue fracture, which originated from the transition R at the installation surface of the connecting rod screw. No metallurgical defects such as slag inclusions or voids were observed on the fracture surface. When checking the size of the transition R on the other side of the connecting rod cover, it was found that there was also a crack about 16mm deep at this position, and the size of the transition R was approximately R2.50. The metallographic structure was a normal tempered bainite structure, and the material of the connecting rod cover met the requirements of 42CrMo in GB/T 3077-2015.

4.3 FEM simulation analysis

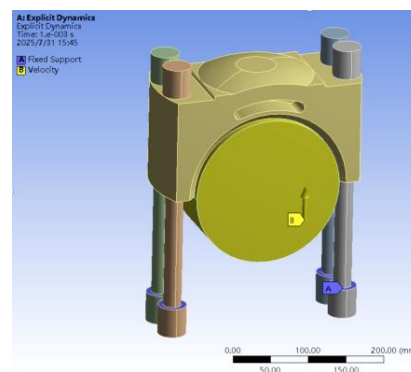
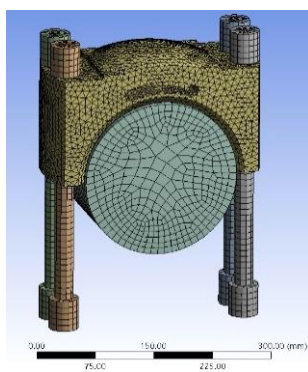
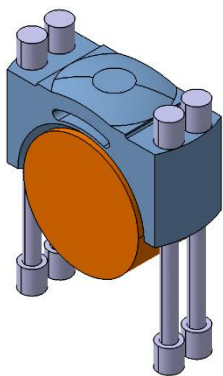


Figure 15: Simplified model.

Figure 16: Mesh generation.

Figure 17: Boundary setting.

Model simplification: In the simulation stage, the free trial versions of ANSYS and CATIA finite element software were mainly used for structural optimization design. The 3D modelling of the connecting rod cover was carried out through the excellent CAD modelling function of CATIA software. The model was imported into the Workbench platform of ANSYS software for finite element analysis. The relevant model simplification referred to the method in reference [1], retaining four connecting bolts for loading, and simplifying the piston, connecting rod, crankshaft, and their connecting parts into one rigid body. The simplified model is shown in Fig. 15.

Meshing settings, constraint and load: The simplified model was meshed. The bolt and crankshaft simplified models were set to the Hex Dominant method, with the maximum limit of related elements within 8 m units. The final meshing resulted in 20,571 nodes and 55,439 elements, as shown in Fig. 16. Constraints were applied to the four bolts and the simplified model, and a rotational speed of 14,400 mm/s was applied to the simplified rigid body according to the compressor's working mode. This rotational speed is much higher than the actual working condition because the research object is a commercial product, and the relevant working conditions are not directly provided. A higher rotational speed also means a higher optimization standard. The relevant settings are shown in Fig. 17.

Simulation results: Under simulation, the stress in the transition area from the bolt installation surface to the inner arc area of the compressor connecting rod cap is significantly greater than the ultimate tensile stress of 902 MPa. Meanwhile, in the simulation results, a fracture failure occurred in the upper right part of the connecting rod cap, with the crack gradually forming from the outer side to the inner side of the cap. The symmetrical area on the left also shows a tendency of fracture failure. After the model fails, the corresponding tensile stress of the connecting bolts also reaches a relatively large state, and subsequent failure due to tensile stress is inevitable. The simplified model is basically consistent with the part's mode and location in the simulation, as shown in Fig. 18.

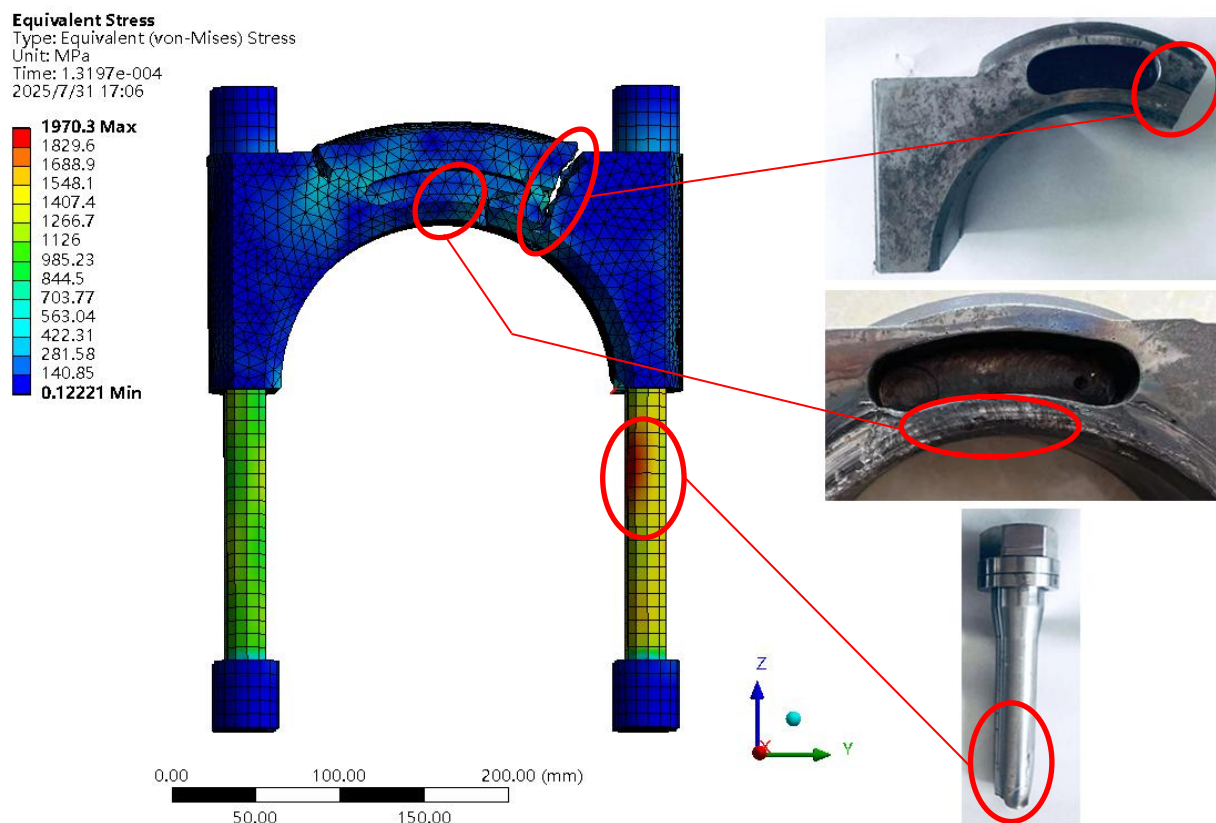


Figure 18: Simulation result.

4.4 Finite element simulation optimization

Based on the part inspection and simulation results, it can be inferred that there is stress concentration in the transition area of the connecting rod cover's bolt installation surface, which leads to the fatigue fracture of the workpiece. Therefore, during the optimization of the part design, this area was optimized. The first optimization scheme increased the fillet radius of the transition area from the original R2.5 to R3.5 and R4.5 respectively; the second

optimization scheme changed the fillet of the transition area to a chamfer, as shown in Fig. 19. The finite element meshing and boundary condition settings for both types of optimization were consistent with the original structure simulation.

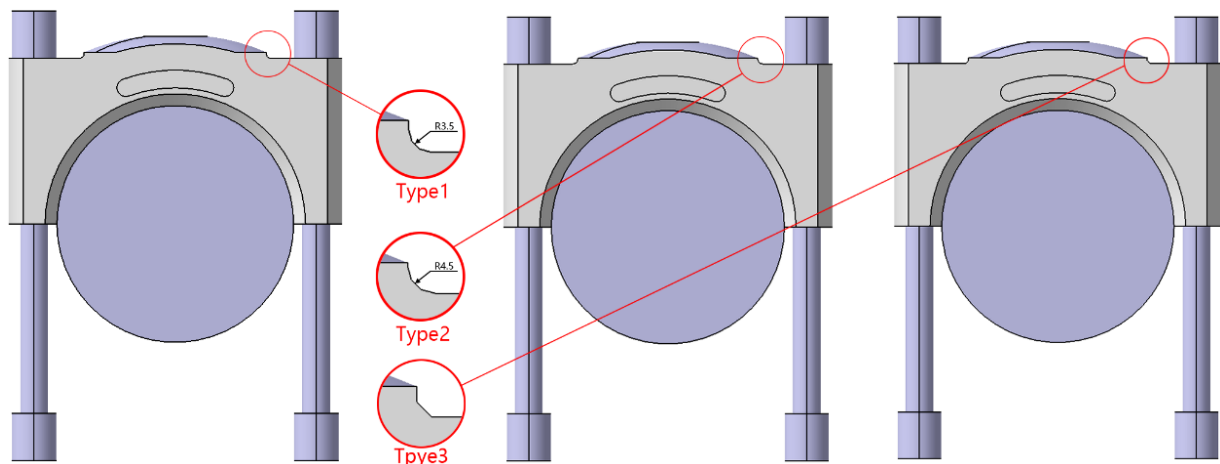


Figure 19: Structural optimization scheme.

The simulation of the R3.5 type structure of the first optimization scheme is shown in Fig. 20. Compared with the original structure, no fracture failure occurred in the transition zone of the cover bolt connection platform, and the stress at this location was around 410 MPa. The stress concentration was significantly improved, effectively reducing the risk of fatigue fracture of the workpiece due to stress concentration.

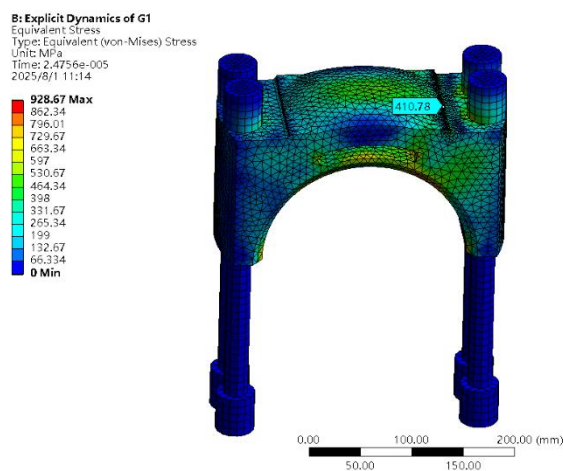


Figure 20: R3.5 simulation.

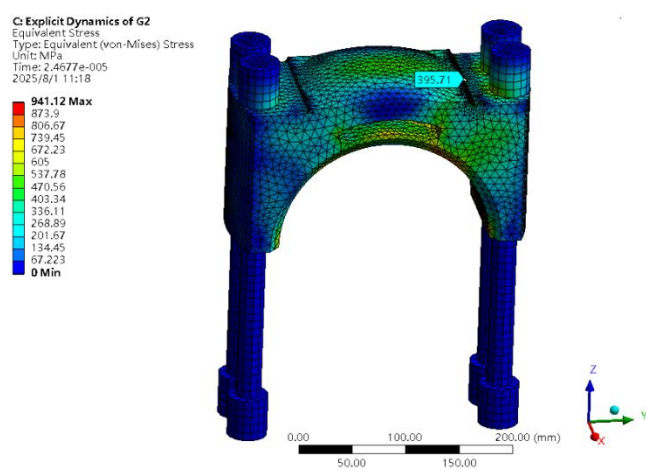


Figure 21: R4.5 simulation.

Further simulation was conducted on the R4.5 type structure, and the results are shown in Fig. 21. Compared with the original structure, no fracture failure occurred in the optimized scheme 2 either. The stress in the transition area of the cover bolt connection plane was further reduced compared with the R3.5 type structure, around 395 MPa, and the stress concentration was further improved. However, the reduction amplitude was slightly weaker than the improvement effect of the R3.5 structure and the original structure.

After replacing the fillet transition structure with the chamfer structure and conducting the simulation again, the results are shown in Fig. 22. Compared with the original structure, although no failure or fracture occurred in this optimized scheme, a fracture crack area still appeared in the transition zone of the cover bolt connection plane. Compared with the fillet

type structure, this kind of structure also has a stress concentration area. Under long-term operation, the parts still have the risk of fracture failure.

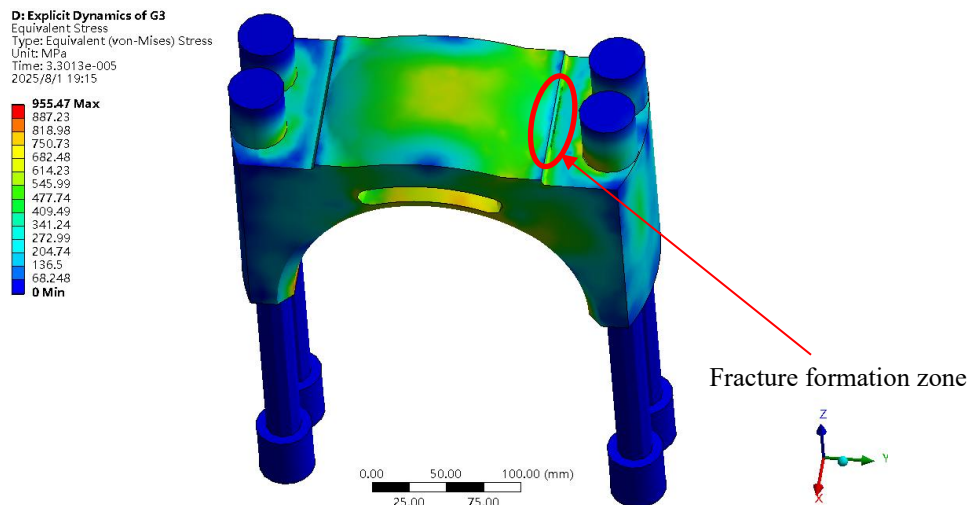


Figure 22: Stress distribution of chamfered structures.

5. CONCLUSION

Based on the above analysis results, the cause of the fracture is that the transition R of the connecting rod screw installation surface is too small. Under actual working conditions, the stress concentration coefficient is too large, which will cause fatigue damage at this position. The accumulation of fatigue damage promotes the formation of fatigue cracks. The fatigue cracks continue to expand during operation until fracture. The final fracture surface shows a typical fatigue origin caused by stress concentration and obvious fatigue expansion arcs in the propagation zone.

Through simulation, it is found that the larger the fillet radius, the more effectively the stress concentration can be improved, and the risk of fatigue fracture can be reduced. However, when it increases to a certain extent, the improvement effect will decrease. A reasonable fillet radius can be selected according to the design. The chamfer structure can reduce the degree of stress concentration, but it cannot completely solve the problem of stress concentration. Under long-term use, fatigue fractures can still occur.

REFERENCES

- [1] Zhu, X.; Xu, J.; Liu, Y.; Cen, B.; Lu, X.; Zeng, Z. (2017). Failure analysis of a failed connecting rod cap and connecting bolts of a reciprocating compressor, *Engineering Failure Analysis*, Vol. 74, 218-227, doi:[10.1016/j.engfailanal.2017.01.016](https://doi.org/10.1016/j.engfailanal.2017.01.016)
- [2] Petrova, I. M.; Filimonov, M. A. (2021). Computational and experimental study of the stress state of the opposed compressor connecting rod to assess the probability of failure-free operation, *Inorganic Materials*, Vol. 57, No. 15, 1505-1510, doi:[10.1134/S0020168521150152](https://doi.org/10.1134/S0020168521150152)
- [3] Wang, D.; Sun, J.; He, Q.; Si, J.; Shi, T.; Li, F.; Xie, K.; Li, W.; Ge, F. (2022). Failure analysis and improvement measures for crankshaft connecting rod of refrigerator compressor, *Engineering Failure Analysis*, Vol. 141, Paper 106585, 11 pages, doi:[10.1016/j.engfailanal.2022.106585](https://doi.org/10.1016/j.engfailanal.2022.106585)
- [4] Çetin, Ö.; Okur, M. (2025). Design and analysis of a crank-connecting rod mechanism without cylinder thrusting for the second stage of a compressor, Vol. 28, No. 6, 1771-1781, doi:[10.2339/politeknik.1569099](https://doi.org/10.2339/politeknik.1569099) (in Turkish)
- [5] Li, X.; Diao, A.; Guo, Y.; Jia, X.; Zhang, C.; Peng, X. (2023). Quantitative diagnosis of loose piston rod threads in reciprocating compressors for hydrogen storage and transport, *International Journal of Hydrogen Energy*, Vol. 48, No. 94, 37013-37030, doi:[10.1016/j.ijhydene.2023.06.032](https://doi.org/10.1016/j.ijhydene.2023.06.032)

- [6] Peng, F.; Huang, Y. (2025). Torsional vibration behavior of compressor shaft system considering variable inertia characteristics of crank-connecting rod mechanisms, *International Journal of Non-Linear Mechanics*, Vol. 170, Paper 104997, 14 pages, doi:[10.1016/j.ijnonlinmec.2024.104997](https://doi.org/10.1016/j.ijnonlinmec.2024.104997)
- [7] Li, T.; Chen, Z.; Zhang, K.; Wang, J.; Huang, Z. (2022). Analysis of the influence of piston–cylinder friction on the torsional vibration characteristics of compressor crankshaft system, *Nonlinear Dynamics*, Vol. 110, No. 2, 1323-1338, doi:[10.1007/s11071-022-07689-9](https://doi.org/10.1007/s11071-022-07689-9)
- [8] Wang, J.; Huang, Z.; Li, J.; Li, T.; Mu, D.; Wang, S. (2023). Analysis of rigid-flexible coupled torsional vibration and vibration suppression of crankshaft system under multiple working conditions, *Proceedings of the Institution of Mechanical Engineers, Part K: Journal of Multi-Body Dynamics*, Vol. 237, No. 4, 710-721, doi:[10.1177/14644193231208532](https://doi.org/10.1177/14644193231208532)
- [9] He, D. X. (2024). Fault prediction in high-efficiency petroleum machinery production, *International Journal of Simulation Modelling*, Vol. 23, No. 1, 184-195, doi:[10.2507/IJSIMM23-1-CO5](https://doi.org/10.2507/IJSIMM23-1-CO5)
- [10] Pang, J. L. (2023). Adaptive fault prediction and maintenance in production lines using deep learning, *International Journal of Simulation Modelling*, Vol. 22, No. 4, 734-745, doi:[10.2507/IJSIMM22-4-CO20](https://doi.org/10.2507/IJSIMM22-4-CO20)
- [11] Hou, C.-C.; Pan, M.-C. (2024). Fault diagnosis of reciprocating compressor using Teager-Kaiser energy operator and envelope spectral feature extraction, *Advances in Mechanical Engineering*, Vol. 16, No. 3, 14 pages, doi:[10.1177/16878132241237638](https://doi.org/10.1177/16878132241237638)
- [12] Kowalczyk, M. J.; Romaniak, A.; Łęcki, M.; Gutkowski, A.; Górecki, G. (2023). Experimental investigation of the energy efficiency of a linear compressor and comparison with a reciprocating compressor in a small refrigeration system, *Archives of Thermodynamics*, Vol. 44, No. 4, 243-260, doi:[10.24425/ather.2023.149723](https://doi.org/10.24425/ather.2023.149723)
- [13] Lu, Y.; Li, Y.; Fu, G.; Jiang, Y.; Huang, Y.; Zhu, J.; Sheng, B. (2024). The physical information LSTM surrogate model for establishing a digital twin model of reciprocating air compressors, *Applied Soft Computing*, Vol. 167, Part A, Paper 112309, 11 pages, doi:[10.1016/j.asoc.2024.112309](https://doi.org/10.1016/j.asoc.2024.112309)
- [14] Elagin, M. Y.; Khmelev, R. N. (2024). Mathematical description of the reciprocating compressor taking into account the influence of suspension parameters on its output characteristics, *Theoretical Foundations of Chemical Engineering*, Vol. 58, No. 4, 1239-1244, doi:[10.1134/s0040579525600056](https://doi.org/10.1134/s0040579525600056)
- [15] Deng, Y.; Jiang, X.; Chuanmin, W.; Bai, L.; Liu, Y.; Hu, K. (2024). Investigation on in-cylinder and in-intercooler thermodynamic properties of miniature multi-stage reciprocating compressor with insufficient inter-stage volumes, *Journal of Thermal Analysis and Calorimetry*, Vol. 149, No. 10, 4691-4708, doi:[10.1007/s10973-024-13028-4](https://doi.org/10.1007/s10973-024-13028-4)
- [16] Kushwaha, D. K.; Panchal, D.; Sachdeva, A. (2025). A modified FMEA approach based integrated decision framework for overcoming the problems of sudden failure and accidental hazards in turbine and alternator unit, *Facta Universitatis, Series: Mechanical Engineering*, Vol. 23, No. 3, Spec. Issue, 459-478, doi:[10.22190/FUME221126010K](https://doi.org/10.22190/FUME221126010K)
- [17] Jankovic, D.; Ristivojevic, M.; Stamenic, Z.; Miskovic, Z.; Dimic, A. (2024). Examination of the causes for premature failure of mating surfaces in smart injector actuators, *Technical Gazette*, Vol. 31, No. 5, 1501-1506, doi:[10.17559/TV-20230403000499](https://doi.org/10.17559/TV-20230403000499)
- [18] Breznikar, Z.; Bojinovic, M.; Brezocnik, M. (2024). Application of machine learning to reduce casting defects from bentonite sand mixture, *International Journal of Simulation Modelling*, Vol. 23, No. 4, 634-643, doi:[10.2507/IJSIMM23-4-702](https://doi.org/10.2507/IJSIMM23-4-702)